Coherent and passive one dimensional quantum memory

2014 New J. Phys. 16 103025

(http://iopscience.iop.org/1367-2630/16/10/103025)

New Journal of Physics
The open access journal at the forefront of physics
Deutsche Physikalische Gesellschaft DPG | IOP Institute of Physics

Coherent and passive one dimensional quantum memory

Yuting Ping[1], John H Jefferson[2] and Brendon W Lovett[1,3]
[1] Department of Materials, University of Oxford, Oxford OX1 3PH, UK
[2] Department of Physics, Lancaster University, Lancaster LA1 4YB, UK
[3] SUPA, School of Physics and Astronomy, University of St Andrews, KY16 9SS, UK
E-mail: bwl4@st-andrews.ac.uk

Received 24 June 2014, revised 28 August 2014
Accepted for publication 10 September 2014
Published 16 October 2014
New Journal of Physics **16** (2014) 103025
doi:10.1088/1367-2630/16/10/103025

Abstract
We show that the state of a flying qubit may be transferred to a chain of identical, (near) ferromagnetically polarized, but non-interacting, static spin-$\frac{1}{2}$ particles in a *passive* way. During this process the flying qubit is coherently polarized, emerging in the direction of the majority static spins. We conjecture that this process is reversible for any number of flying qubits injected sequentially in an arbitrary superposition state, proving this explicitly for an arbitrary state of one and two flying qubits. We also find a special case in which we are able to prove the conjecture for an arbitrary number of qubits. Our architecture thus has the potential to be exploited as a passive quantum memory to encode the flying qubits without the necessity of resetting between successive encoding operations. We also illustrate that the quantum information may be spread over many static spins in the memory chain, making the mechanism resistant to spin decoherence and other imperfections. We discuss implementing the memory system with trapped bosonic atoms, controlled by a spatial light modulator.

Keywords: spin chain, quantum memory, decoherence

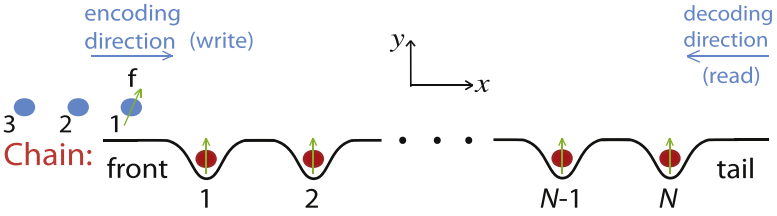

Figure 1. Illustration of the passive memory system (not to scale) with the associated QST scheme. The coherent quantum memory consists of a sufficiently long, ferromagnetically polarized chain $|F\rangle$ of non-interacting, static spins (red). Each flying qubit (blue) enters the front end of the chain, interacts with the static spins sequentially and eventually emerges as polarized $|\uparrow\rangle_f$ at the tail end. The chain can then encode subsequent flying qubits sequentially in the same fashion. To read out from the memory, one simply injects a polarized qubit $|\uparrow\rangle_f$ back from the tail, and the state of the last encoded flying qubit is then recovered automatically out from the front. More states can be recovered sequentially in the same way by further injecting back polarized qubits $|\uparrow\rangle_f$ from the tail. There is no need to reset between successive encoding (decoding) rounds. Any multi-partite entanglement between injected qubits is also recovered in the read operations.

1. Introduction

Robust quantum state transfer (QST) plays an important role in the field of quantum information processing (QIP), achieving quantum transmission of data through space or time [1]. Over the past decade numerous efforts have been made in this area, and many potentially feasible approaches have been suggested for both state transportation [2] and storage [3–7] in a variety of physical systems. However, in most instances, exercising the required level of active quantum control remains a challenging aspect of the current technology: errors are most likely introduced. On the other hand, it has recently been proposed that schemes utilizing iterative applications of quantum maps can perform certain QIP tasks with reduced level of quantum control [8, 9].

In this paper, we work with an iterative setting for a coherent quantum memory under limited quantum control. We imagine that quantum states are transported by qubits which are mobile (called 'flying qubits'), and can move from one quantum processor to another. The challenge then is to 'catch' such qubits, such that their states might be stored statically, i.e. in the location of the processor, in a register of long lived quantum memory elements. We will here describe a method for enabling such an operation. We will show that it is possible to sequentially transfer the states of a number of flying qubits to a long memory chain of N identical, ferromagnetically polarized, but non-interacting, static spins in a *completely passive* way (see figure 1).

In the next section we introduce our spin chain model and discuss encoding a single flying qubit in it. In section 3 we discuss decoherence and operational errors in the single qubit memory, before in section 4 showing how our ideas can be extended to multiple flying qubits. We show how to implement our model in a real system in section 5 before concluding in section 6.

2. Single qubit quantum memory

2.1. Encoding of spin information

We start by considering a flying qubit in some arbitrary state $|\psi\rangle_{f_1} = \alpha\,|\uparrow\rangle + \beta\,|\downarrow\rangle$ with the static spins in the state $|F\rangle_c = |\uparrow_{s_1} \ldots \uparrow_{s_N}\rangle$. As shown in figure 1, during encoding $|\psi\rangle_{f_1}$ enters from the front into the chain and interacts with the static spins s_1–s_N sequentially. We model the interactions by an effective Hamiltonian coupling each flying qubit (f_i) and the kth static spin of the following form

$$H_k^i(t) = \frac{g_k^i(t)}{2}\left(\sigma_{f_i}^x\sigma_{s_k}^x + \sigma_{f_i}^y\sigma_{s_k}^y\right) = g_k^i(t)\left(\sigma_{f_i}^+\sigma_{s_k}^- + \sigma_{f_i}^-\sigma_{s_k}^+\right), \tag{1}$$

where $\sigma^{\pm} = (\sigma^x \pm \mathrm{i}\sigma^y)/2$ are Pauli spin–flip operators. The g_k^i are the XY exchange coupling strengths that depend on the separation of the ith qubit and the spin s_k. As the mobile spin moves along and approaches a spin in the chain, the strength of its interaction with that spin increases, before decreasing again after it has moved past. We are able to capture this behaviour by assuming that the g_k^i are time dependent, effectively being controlled by the motion of the flying spin. Indeed, we have checked that such a time dependent interaction can be reproduced by starting from a static Hamiltonian with an appropriate initial condition, and solving the scattering problem, see appendix A.

For the general state $|\Psi_k^i(t)\rangle = U_k^i(t)|\Psi_k^i(0)\rangle$ of the qubit f_i and the spin s_k, we have the time evolution operator $U_k^i(t) = \exp\,[-\mathrm{i}\theta_k^i(t)(\sigma_{f_i}^+\sigma_{s_k}^- + \sigma_{f_i}^-\sigma_{s_k}^+)]$, with $\theta_k^i(t) = \int_0^t g_k^i(t')\mathrm{d}t'/\hbar$. Let us assume that the flying spin is initially far enough away that $g_k^i(0)$ is negligible. Then as time progresses it approaches the static spin and so the interaction strength increases and reaches a maximum at closest approach, before decreasing and becoming negligible again by time τ. Then we find that the total effect of a static–flying spin interaction is captured by the unitary operator $U_k^i = \exp\,[-\mathrm{i}\theta_k^i(\sigma_{f_i}^+\sigma_{s_k}^- + \sigma_{f_i}^-\sigma_{s_k}^+)]$ with $\theta_k^i = \int_0^\tau g_k^i(t')\mathrm{d}t'/\hbar$, now independent of time. In the basis $\{|\uparrow_{f_i}\ \uparrow_{s_k}\rangle, |\uparrow_{f_i}\ \downarrow_{s_k}\rangle, |\downarrow_{f_i}\ \uparrow_{s_k}\rangle, |\downarrow_{f_i}\ \downarrow_{s_k}\rangle\}$

$$U_k^i = \begin{pmatrix} 1 & 0 & 0 & 0 \\ 0 & \cos\theta_k^i & -\mathrm{i}\sin\theta_k^i & 0 \\ 0 & -\mathrm{i}\sin\theta_k^i & \cos\theta_k^i & 0 \\ 0 & 0 & 0 & 1 \end{pmatrix}, \tag{2}$$

where in general we will consider $\theta_k^i = \theta \in (0, \pi/2]\ \forall\ \ k,\ \ i$[4].

Starting from the total state $|\psi, F\rangle = |\psi\rangle_{f_1}|F\rangle_c$, we apply U_k^1 as in equation (2) to the flying qubit and the kth static spin sequentially for s_1 through to s_N. The state $|\uparrow, F\rangle$ with amplitude α remains the same during this write operation, while $|\downarrow, F\rangle$, with amplitude β, evolves as follows

[4] We note that for the *Heisenberg* model, there would be an extra term $\frac{g_k^i}{2}\sigma_z^{f_i}\sigma_z^{s_k}$ in equation (1), and U_k takes the same form apart from an extra phase factor of $\mathrm{e}^{\mathrm{i}\theta_k^i}$ for each trigonometric term. We find however, that the different symmetry of this model means that the memory only works well for $\theta^i = \pi/2$.

$$
\begin{aligned}
|\downarrow, F\rangle \Rightarrow_1 & \cos\theta\ \underline{|\downarrow, F\rangle} - \mathrm{i}\sin\theta\ \sigma_1^-\,|\uparrow, F\rangle \\
\Rightarrow_2 & \cos\theta\left(\cos\theta\ \underline{|\downarrow, F\rangle} - \mathrm{i}\sin\theta\ \sigma_2^-\,|\uparrow, F\rangle\right) - \ \mathrm{i}\sin\theta\ \sigma_1^-\,|\uparrow, F\rangle \\
\Rightarrow_k & \ \ldots\ \ \forall\ \ k = 3,\ldots,N-1 \\
\Rightarrow_N & -\mathrm{i}\sin\theta\sum_{k=1}^{N}\cos^{k-1}\theta\ \sigma_k^-\,|\uparrow, F\rangle + \overset{0 \text{ as } N\to\infty}{\cancel{\cos^N}\ \theta}\,|\downarrow, F\rangle
\end{aligned}
\tag{3}
$$

where $\Rightarrow_k$ corresponds to the occurrence of an interaction event for the flying qubit with the static spin s_k, and we switch from the cumbersome notation $\sigma_{s_k}^-$ to the more compact σ_k^- to denote a static spin down-flip in the kth position of the chain (flying spins will continue to be denoted using the f subscript). Note that the only component which evolves further in each superposition is underlined in equation (3). Combining both parts, we see that the flying qubit emerges as polarized $|\uparrow\rangle_{f_1}$ with probability $1 - \cos^{2N}\theta \to 1$ for $N \to \infty$. In this limit, the initial quantum information which $|\psi\rangle_{f_1}$ held before encoding has now been transferred to the chain, whose collective state reads

$$
\left(\alpha - \mathrm{i}\beta\sin\theta\sum_{k=1}^{N\to\infty}\cos^{k-1}\theta\ \sigma_k^-\right)|F\rangle. \tag{4}
$$

The probability of a single down-flip at site k is $|\beta|^2\sin^2\theta\cos^{2(k-1)}\theta$, a quantity that decays exponentially along the chain. Summing over all these probabilities gives $|\beta|^2$, as expected by conservation of total probability.

2.2. Decoding the memory qubit

To read out the state $|\psi\rangle$ of the original flying qubit from the memory, we inject a polarized flying qubit $|\uparrow\rangle_f$ from the tail back to the chain, i.e., in the opposite direction as for the encoding operation (see figure 1). This is the simplest decoding method for the memory system, and it requires the flying readout qubit to have the same kinetic energy as the encoded flying qubit.

Just before the read operation, the total state of the flying qubit and the chain is

$$
\left(\alpha - \mathrm{i}\beta\sin\theta\sum_{k=1}^{N\to\infty}\cos^{k-1}\theta\ \sigma_k^-\right)|\uparrow, F\rangle. \tag{5}
$$

The state $|\uparrow, F\rangle$ with amplitude α again remains the same during decoding, while each state $\sigma_k^-\,|\uparrow, F\rangle$, with amplitude $-\mathrm{i}\beta\sin\theta\cos^{k-1}\theta$, evolves as follows, as the flying spin passes each member of the chain

$$
\begin{aligned}
\sigma_k^-\,|\uparrow, F\rangle \Longrightarrow_{N(\to\infty)} & \ldots \Longrightarrow_{k+1}\sigma_k^-\,|\uparrow, F\rangle \\
\Longrightarrow_k & \quad \cos\theta\ \sigma_k^-\,|\uparrow, F\rangle - \mathrm{i}\sin\theta\,\underline{|\downarrow, F\rangle} \\
\Longrightarrow_{k-1} & \quad \cos\theta\ \sigma_k^-\,|\uparrow, F\rangle - \mathrm{i}\sin\theta\left(\cos\theta\,\underline{|\downarrow, F\rangle} - \mathrm{i}\sin\theta\sigma_{k-1}^-\,|\uparrow, F\rangle\right) \\
\Longrightarrow_{k'} & \quad \ldots\ \forall\ k' = k-2,\ldots,2 \\
\Longrightarrow_1 & \quad \cos\theta\ \sigma_k^-\,|\uparrow, F\rangle - \mathrm{i}\sin\theta\cos^{k-1}\theta\,|\downarrow, F\rangle
\end{aligned}
$$

$$- \sin^2\theta \sum_{j=1}^{k-1} \cos^{j-1}\theta \ \sigma_{k-j}^{-} \,|\uparrow, F\rangle \quad \text{if } k \geqslant 2$$
$$\text{or } \cos\theta \ \sigma_1^{-} \,|\uparrow, F\rangle - \mathrm{i}\sin\theta \,|\downarrow, F\rangle \quad \text{if } k = 1. \tag{6}$$

Thus, by linearity, the total state after decoding becomes

$$\begin{aligned}
&\alpha \,|\uparrow, F\rangle - \mathrm{i}\beta \sin\theta\big(\cos\theta \ \sigma_1^{-} \,|\uparrow, F\rangle - \mathrm{i}\sin\theta \,|\downarrow, F\rangle\big) \\
&-\mathrm{i}\beta \sin\theta \sum_{k=2}^{\infty} \cos^{k-1}\theta\Big(\cos\theta \ \sigma_k^{-} \,|\uparrow, F\rangle - \mathrm{i}\sin\theta\cos^{k-1}\theta \,|\downarrow, F\rangle\Big) \\
&+\mathrm{i}\beta \sin\theta \sum_{n=2}^{\infty} \cos^{n-1}\theta\left(\sin^2\theta \sum_{j=1}^{n-1} \cos^{j-1}\theta \ \sigma_{n-j}^{-} \,|\uparrow, F\rangle\right),
\end{aligned} \tag{7}$$

where in the last line we have replaced the dummy variable k by n. By absorbing the bracketed terms in the first line into the summation of the second line, equation (7) is equivalent to

$$\begin{aligned}
&\left(\alpha \,|\uparrow, F\rangle - \beta \underbrace{\sin^2\theta \sum_{k=1}^{\infty} \cos^{2(k-1)}\theta}_{1} \,|\downarrow, F\rangle\right) - \mathrm{i}\beta \sin\theta \\
&\times\left(\sum_{k=1}^{\infty} \cos^{k}\theta \ \sigma_k^{-} - \sin^2\theta \sum_{n=2}^{\infty}\sum_{j=1}^{n-1} \cos^{n+j-2}\theta \ \sigma_{n-j}^{-}\right)|\uparrow, F\rangle,
\end{aligned} \tag{8}$$

where the first sum is simply a geometric series. For the double summation we want to focus on the coefficients for σ_k^{-}, and hence the sum over j can be replaced by a sum over k with $k = n - j \geqslant 1$, i.e.

$$\begin{aligned}
\sum_{n=2}^{\infty}\sum_{j=1}^{n-1} \cos^{n+j-2}\theta \ \sigma_{n-j}^{-} &= \sum_{k=1}^{\infty}\sum_{n=k+1}^{\infty} \cos^{2(n-1)-k}\theta \ \sigma_k^{-} \\
&= \sum_{k=1}^{\infty} \frac{\cos^{k}\theta}{\underbrace{1 - \cos^2\theta}_{\sin^2\theta}} \ \sigma_k^{-},
\end{aligned} \tag{9}$$

where we have swapped the double summations as the sum over n runs to infinity. Therefore, the second line in equation (8) becomes zero due to complete cancellations for each $k = 1, 2, \ldots \infty$, and the total state after decoding is then simply

$$(\alpha \,|\uparrow\rangle - \beta \,|\downarrow\rangle)_f \otimes |F\rangle_c. \tag{10}$$

As a result, after the read operation the chain returns to the original ferromagnetically polarized state and is disentangled from the flying qubit, which now emerges out from the front of the chain as $\sigma_f^z|\psi\rangle_{f_1} = \alpha \,|\uparrow\rangle - \beta \,|\downarrow\rangle$. That is, we recover the original state of the flying qubit, up to a phase flip which can be corrected by a σ_f^z gate [11, 12].

2.3. Resource scaling

To see how the size N of the memory chain required to store one qubit scales with the coupling strength θ, we use the condition that $\cos^{2N}\theta \to 0$ for sufficiently large N. Given an error tolerance $\epsilon > 0$ such that $\cos^{2N}\theta < \epsilon$, we require

$$2N(\theta) > \frac{\ln \epsilon}{\ln \cos \theta} \approx -\frac{2 \ln \epsilon}{\theta^2} (\theta \ll 1). \tag{11}$$

The required memory size thus increases significantly with decreasing θ for fixed ϵ. For example, with $\epsilon \sim 10^{-4}$ and $\theta = 1$, $N_{\min} \simeq 8$ rising to ~920 for $\theta = 0.1$. However, in the weak coupling regime, each static spin contains only a fraction of the qubit's state, and so has the potential to store more. On the other hand, for stronger couplings a relatively short chain can already store a number of flying qubits. In the special case where $\theta = \frac{\pi}{2}$, one polarized static spin in the chain is sufficient to store a flying qubit, since now U_k^i in equation (2) is simply a $SWAP_k^i$ gate (up to a phase of '$-i$').

3. Single qubit decoherence and operational errors

In this section we will look in detail at how robust our protocol is to various imperfections, covering both environmental decoherence in section 3.1 and imperfect operation in section 3.2.

3.1. Decoherence

We consider the effect of decoherence on a chain in which one qubit state $|+\rangle_{f_1} = (|\uparrow\rangle_{f_1} + |\downarrow\rangle_{f_1})/\sqrt{2}$ is stored; the chain state is described by equation (4) with $\alpha = \beta = 1/\sqrt{2}$. Both the write and the read operations are assumed to be fast, and the principal effect of decoherence is on the static spins for the time (τ) during which the qubit is stored in the chain. We model this with a standard Lindblad master equation [13]

$$\dot{\rho} = \sum_{i=1}^{N} \Gamma_i \left(L_i \rho L_i^\dagger - \frac{1}{2}\left(L_i^\dagger L_i \rho + \rho L_i^\dagger L_i \right) \right), \tag{12}$$

where ρ is the density matrix of the memory, and the L_i are the noise operators with noise rates Γ_i; the usual unitary term is omitted since we are only interested in the storage period. Restricting to the subspace consisting of only zero or one excitations among the static spins, we have simulated the behaviour of a memory chain of fixed length $N = 100$ under dephasing errors ($L_i = \sigma_i^z$). We vary θ such that the qubit is stored in the first N_s ($\leqslant N$) number of static spins with $\epsilon \sim 10^{-2}$ (see equation (11)), to monitor the effect of spreading the quantum information stored in the memory.

We find that for homogeneous dephasing, in which each spin is subject to the same, independent decoherence process, the total decoherence for the memory is essentially the same for all θ. In our simulations we take a dephasing rate $\Gamma_i = 1\,\mathrm{MHz}$ for each static spin and each resulting fidelity of the recovered qubit as a function of time always coincides exactly with the red curve in figure 2(a), regardless of the chosen $N_s \leqslant N$. The decoherence rate does not therefore depend on how local or distributed the information is in the quantum memory, since the relevant qubits which contain the quantum information each decohere at the same rate. In other words, even though for a larger N_s there is less information stored on each chain spin,

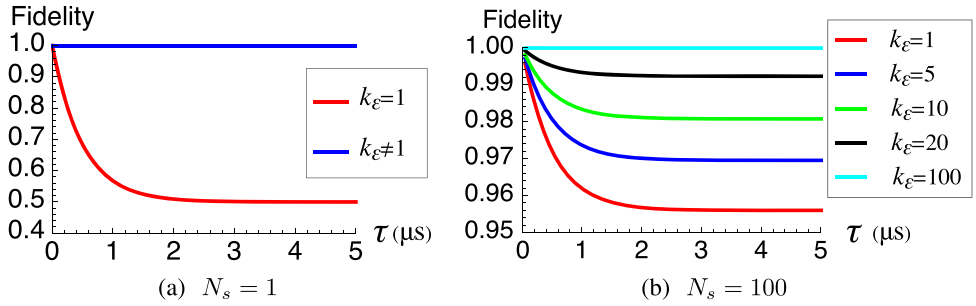

Figure 2. Plots for the fidelity of the retrieved qubit, relative to the input $|+\rangle_{f_1}$, against the storage time τ under inhomogeneous dephasing with rate $\Gamma_k = 1$ MHz (coherence time 1 μ s) for the k_εth static spin and *zero* for all others ($N = 100$). We vary θ such that the qubit is stored in the first N_s number of static spins with $\epsilon \sim 10^{-2}$ by equation (11): (a) The qubit is stored entirely in the first qubit ($\theta = \pi/2$). (Note that the red curve here coincides exactly with the fidelity curve obtained under a homogeneous dephasing model for any N_s with rate $\Gamma_k = 1$ MHz across all spins, as discussed in the text.) (b) The whole chain of 100 spins store the qubit collectively ($\theta \simeq 0.30$).

there are also more information carrying spins that are subject to decoherence. The two effects cancel, and we are left with no dependence on N_s. It also follows that the fidelity must eventually saturate to $\frac{1}{2}$ when all the memory qubits lose their quantum information.

On the other hand, for inhomogeneous decoherence processes in which the spins decohere at different rates, distributing the quantum information does reduce the variance of the total memory decoherence rate compared with locally stored information, and this difference can be very large. We illustrate this in figure 2(b) for the case when just one static spin is subject to decoherence (for example due to the proximity of a magnetic impurity). When the quantum information is stored locally (in the first qubit with $\theta = \frac{\pi}{2}$ in figure 2(a)) then the fidelity F saturates to $\frac{1}{2}$ when the decohering spin is the first, whereas $F = 1$ if the decohering spin is any of the other $N-1$ spins. The former case has a fidelity curve which exactly matches those for the homogeneous case discussed above, since the only relevant decoherence process is that acting on the first spin—it is thus the $N_S = 1$ limit of the homogeneous set of curves. However, when the quantum information is spread over all N spins ($\theta \simeq 0.30$ in figure 2(b)), the saturated fidelity becomes $\gtrsim 1 - \frac{1}{2N}$, independent of which spin is subject to decoherence. This result may easily be extended to cases when more than one spin decoheres, or the spins decohere at different rates. Spreading the information over many qubits *smooths* the statistical fluctuations in information loss.

3.2. Imperfect operation

Here we consider what happens if the read-out operation is imperfect—i.e. if the kinetic energy of the flying qubit during the read operation differs from that of the input for encoding (i.e., $\theta_{\rm dec} \neq \theta_{\rm enc}$). We numerically simulate how the error affects the memory for various chain lengths N in figure 3, where $\chi = (\theta_{\rm dec} - \theta_{\rm enc})/\theta_{\rm enc}$. Here, $\theta_{\rm enc}$ is adjusted so that each chain with length N is just enough to collectively store the qubit (defined by setting $\cos^N\theta_{\rm enc} = 0.01$).

From figure 3, we see that after the decoding round, the retrieved qubit is of a high fidelity ($\geqslant$99%) with respect to the original input, for small mismatches ($\sim$10%) in the encoding and

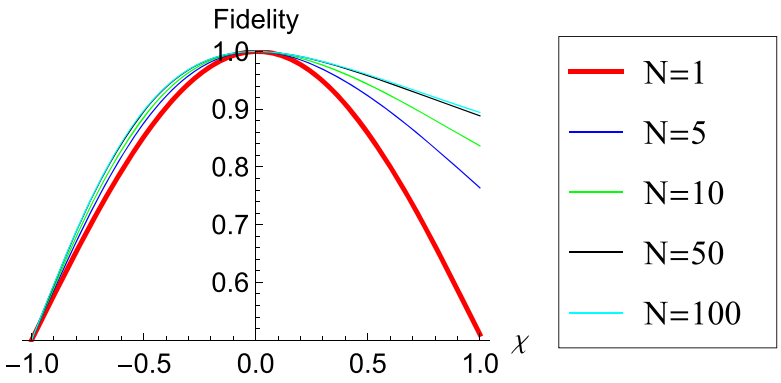

Figure 3. Plots of the fidelity of the retrieved qubit, relative to the input $|+\rangle_{f_1}$, against the fractional difference χ between the coupling strengths during encoding (θ_{enc}) and decoding (θ_{dec}), for various chain lengths. For each N, the whole chain collectively stores the qubit, i.e., $N_s = N$.

decoding θ values. Moreover, as the number N of static spins increases, the memory's tolerance to such errors improves.

4. Encoding multiple qubits

In this section we extend our analysis of the storage capability of the chain to more than one qubit. The general proof that it is possible to both encode and decode an arbitrary number of input flying qubits with arbitrary multi-particle superpositions remains presently a conjecture, but we have strong evidence that it is true. In particular, we have been able to extend our proof from one to two flying qubits, thus including entangled states, as well as to the case where there is only one $|\downarrow\rangle_f$ among any number of flying $|\uparrow\rangle_f$ qubits. We have also performed numerical simulations for various states of four qubits, and we will show that the memory faithfully stores such states, and that they can be retrieved with high fidelity.

4.1. Analytical proof for a two qubit memory

The proof that two flying qubits can be stored is described in detail in appendix B, whereas in appendix C, we prove that one $|\downarrow\rangle_f$ among any number of flying $|\uparrow\rangle_f$ qubits can also be stored and retrieved. Here we will simply outline some essential ingredients of these proofs.

For the second proof (appendix C), we have to define a 0th collective one-spin down-flip operator on the chain $|F\rangle_c$ arising from equation (3)

$$D_0^{(1)} = \sum_{k=1}^{\infty} a_0^{(1)}(k)\, \sigma_k^- := \sum_{k=1}^{\infty} \left(-\mathrm{i}\, \sin\theta\, \cos^{k-1}\theta\right) \sigma_k^-. \tag{13}$$

We find $\sum_k |a_0^{(1)}(k)|^2 = 1$, as expected for unit total probability. We then show that this chain distribution can be altered by further storing l subsequent $|\uparrow\rangle_f$ qubits, resulting in the lth collective one-spin down-flip

$$D_l^{(1)} = \sum_{k=1}^{\infty} a_l^{(1)}(k)\ \sigma_k^- \tag{14}$$

with

$$\begin{aligned} a_l^{(1)}(k) &= a_0^{(1)}(k) \sum_{r=0}^{\min\{l,k-1\}} (-1)^r \binom{k-1}{r}\binom{l}{r} \tan^{2r}\theta\, \cos^l\theta \\ &= a_0^{(1)}(k)\ {}_2F_1\left(1-k, -l; 1; -\tan^2\theta\right)\ \cos^l\theta, \end{aligned} \tag{15}$$

where the more compact form ${}_2F_1(a, b; c; z)$ denotes the *Gauss* hypergeometric function [14]. Similarly, we are able to decode the stored qubits in the reverse order (see appendix B and appendix C). It follows that the memory chain can store two-qubit states $|\uparrow_{f_1}\ \downarrow_{f_2}\rangle, |\downarrow_{f_1}\ \uparrow_{f_2}\rangle$, which can be read out sequentially.

We have also proved that encoding and decoding two $|\downarrow\rangle_f$ qubits in the chain $|F\rangle_c$ can be done in a similar fashion (see appendix C), with the (0, 0)th collective two-spin down-flip amplitude after encoding being

$$a_{(0,0)}^{(2)}(k_1, k_2) = (-\mathrm{i}\sin\theta)^2\left(2 - (k_2 - k_1 - 2)\tan^2\theta\right)\cos^{k_1+k_2-1}\theta. \tag{16}$$

By linearity (combining with the results from equation (15)), the memory can thus store at least two qubits of arbitrary states, including any bipartite entanglement (and hence qubits of mixed states).

4.2. Many qubits

To generalize the above analytical proof for one and two flying qubits to many qubits we would need to show that the chain can store a spin state that includes an arbitrary number n of down-spins

$$D_{(l_1,\ldots,l_n)}^{(n)} = \sum_{k_1<\ldots<k_n} a_{(l_1,\ldots,l_n)}^{(n)}(k_1,\ldots,k_n)\ \sigma_{(k_1,\ldots,k_n)}^-, \tag{17}$$

where the k_is denote the spin–flip positions and l_i denotes the number of $|\uparrow\rangle_f$ encoded between the ith and $(i+1)$th flying $|\downarrow\rangle_f$ qubits. This would mean that the chain can store a number of flying qubits, each of which was originally either $|\uparrow\rangle_f$ or $|\downarrow\rangle_f$ and can be further retrieved by the aforementioned decoding mechanism. Arbitrary multi-particle superpositions and entanglement then follows by linearity. Unfortunately, this procedure becomes impractical for more than two down-spins due to the difficulty of keeping track of all the indices, and a rigorous proof for an arbitrary number of up-spin and down-spin qubits remains an open challenge.

However, for the special case of $\theta = \pi/2$ the write and read operations are much simplified since each flying–static qubit interaction is a simple exchange of spins, as seen directly from equation (2), with an extra factor $(-i)$ when the spins are antiparallel. As a consequence of this the write operation involves only the first n qubits of the static array, where n is the number of incident flying qubits. This greatly alleviates the problem of tracking the states and their phases as the flying qubits propagate through the static array, enabling an expression to be derived for the chain spin state after the 'write' operation—and an analytical proof that the original flying qubit state is recovered after the read operation can then also be found. Details of this are given

in appendix D, and these results add further support for the basic conjecture for arbitrary θ. This special case could of course itself be used as a quantum memory though is more prone to errors than the case with small θ for which the quantum information is spread over many static qubits after the write operation.

We conclude this section by pointing out some similarities and differences with earlier work on a 'quantum homogeniser' [10], whose function is to imprint the state of a set of identically prepared static spins onto that of a *single* flying spin. Moreover, following interaction, all the spins (static and flying) are meant to be close to the original state of the static spins—hence the term 'homogeniser'. By contrast, in our work the focus is on coherent and ordered sequential interaction and how this may be used to realize a quantum memory for multiple spins. We find that whilst the spins of the static qubits in the 'tail' of the chain will be approximately aligned following encoding, this is not necessarily the case near the 'head' of the chain where their mean spin directions can change considerably after interaction. An extreme example is that of n down-spin flying qubits with $\theta = \pi/2$ as described above and in appendix D. In this case, after all interactions have taken place, the first n static qubits have spin down with the remainder spin up, and the flying qubits emerge with spin up: a clearly inhomogeneous situation. We also note that even though it was realized in [10] that encoded information about the flying spin could be retrieved if it were possible to reverse the time evolution of the encoding, a physical operation to do this is not proposed there. We have here explained how decoding can be performed, shown how multiple qubits can be stored and retrieved, and discussed the coherence properties of the device.

4.3. Numerical simulations

A numerical check of our two qubit proof, for $N = 8$ static spins, is shown in figure 4, demonstrating that the state can be retrieved with high fidelity and errors within the expected limits.

Importantly, we are able to provide further support for the conjecture that the memory chain works for more than two qubits using numerical simulations as shown in figure 5(a). The simulation exploits a short ($N = 9$) chain with four flying qubits of randomly generated states. θ is assumed to take the same value across the whole register, and chosen to give a high probability for a ferromagnetically aligned tail after encoding. Analysis of the fidelity after decoding gives results which are consistent with the conjecture within the expected error bounds.

We also extend this analysis to the case where four randomly-generated, pure qubits each have a different kinetic energy. To separate the effects of this from that of having a finite chain length, we employ the same qubits $\{\rho_i\}_4$ as generated in the simulations of figure 5(a) and simulate their storage and retrieval from the memory $|F\rangle_c$ with the same length $N = 9$, but with random $\theta^i \in (0.9, 1.1)$ for each i. Each θ_i matches for the corresponding decoding and encoding operations of ρ_i (effects of such mismatches were shown earlier in figure 3); site-to-site variations are also ignored, but considered below. Figure 5(b) thus illustrates the effects of small round-to-round variations ($\sim\pm 10\%$) in the coupling strengths θ^i, and shows that the memory is robust towards such imperfections as long as the memory has sufficient capacity to store each qubit reliably (i.e., has a large enough N).

We next consider site-to-site variations in θ_k. We encode and decode one qubit ρ_1 into the chain $|F\rangle_c$ with $N = 9$, with variable coupling strengths $\theta_k \in (0.9, 1.1)$ between the qubit and

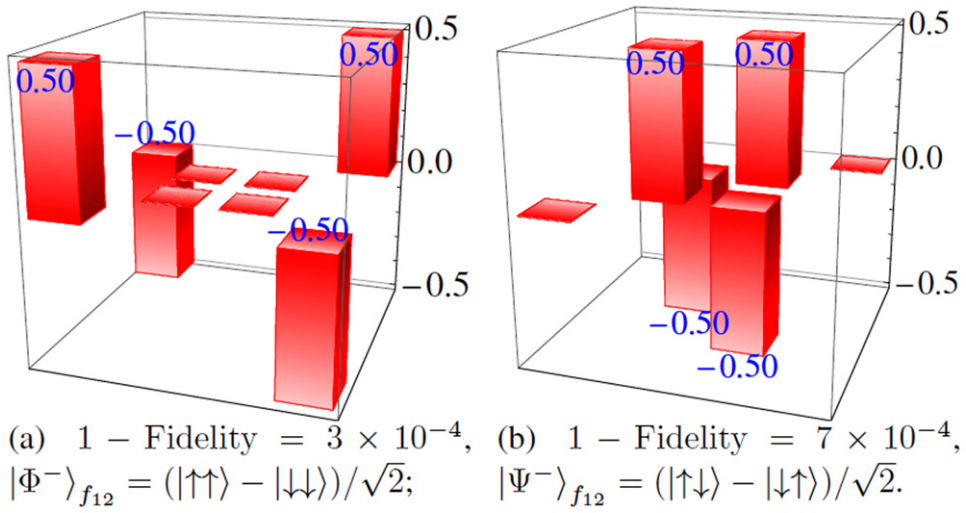

Figure 4. Density state tomograms constructed for the corresponding, retrieved (two-qubit) quantum state from a memory chain $|F\rangle_c$ consisting of $N = 8$ static spins without decoherence. (a) and (b) represent two *separate* cases of memory storage and retrieval of quantum information. The inputs, both entangled, are indicated in each case, together with the corresponding infidelity of the retrieved state. We chose a non-special value $\theta = 1.1$; for a tolerance $\epsilon \sim 10^{-4}$, this requires $N \geqslant 6$ to reliably store one qubit, as predicted by equation (11).

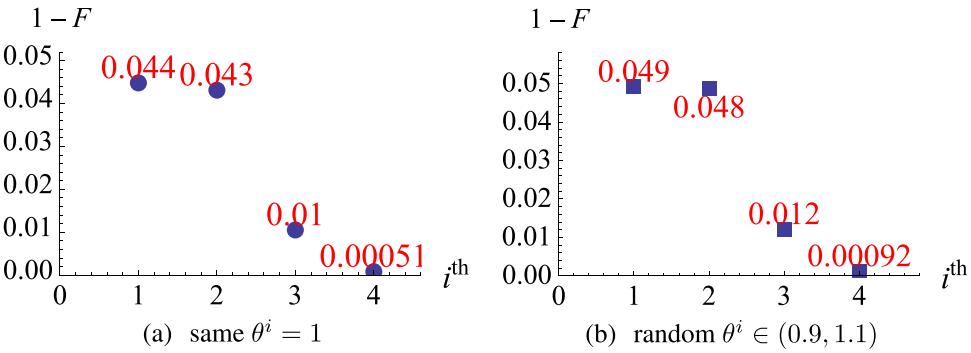

Figure 5. Plots for the infidelity $1 - F$ of the retrieved qubit (with phase corrected), relative to the corresponding input ρ_i, against the ordinal number i of the inputs. Here, four randomly-generated pure qubits $\{\rho_i\}_4$ are sequentially encoded into the memory chain $|F\rangle_c$ ($N = 9$), and then retrieved one by one in the reverse order without decoherence. (a) Here we assume a uniform $\theta = 1$, and hence for $\epsilon \sim 10^{-4}$ (or 10^{-2}) it requires $N \geqslant 7$ (or 4) to reliably store one qubit. The finite chain length restricts the number of qubits the memory can hold; within its capacity the last encoded (or the first retrieved) qubit always has the highest fidelity, since part of the quantum information stored for the earliest qubits may have been 'pushed out' of the memory by the later ones during encoding. (b) Here θ is assumed to vary randomly in each round, between the two values indicated (site-to-site variations are neglected). Ten independent runs of simulations are performed, and for each qubit the average is taken for the phase-corrected fidelity (to discount the imperfect randomness in θ^i for small number of rounds n and hence possible outliers).

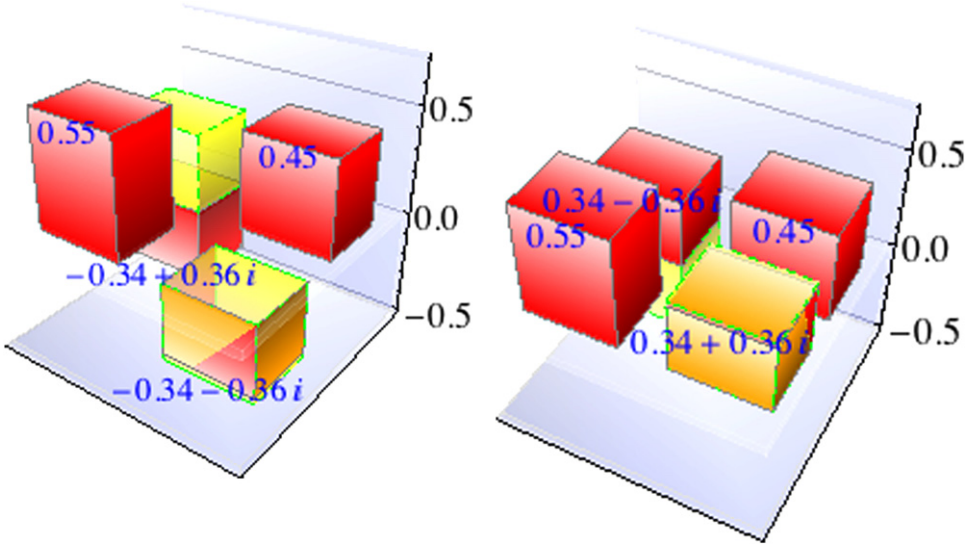

(a) ρ_1 (b) ρ_1^{ret}

Figure 6. Density state tomograms ('red' for real components and 'yellow' for imaginary) constructed for (a) the input ρ_1 generated above (i.e., from the main text); (b) the retrieved qubit ρ_1^{ret}, by encoding *only* ρ_1 into the the memory chain $|F\rangle_c$ (with $N = 9$) and then read back (without correcting the phase). We have random $\theta_k \in (0.9, 1.1)$ between the qubit and the kth static spin. The infidelity of the retrieved qubit, if phase corrected, is 7.4×10^{-6}, which is again averaged over the results from ten independent runs of simulations. For comparison, the corresponding infidelity for $\theta_k = 1\ \forall\ k$ is 6.1×10^{-6}.

kth static spin. Note that again θ_k matches for the decoding and encoding operations for the same position k. In this case, we found the infidelity (averaged over ten independent runs) between ρ_1^{ret} and ρ_1 to be $\sim 10^{-6}$, similar to that in the case of $\theta_k = 1\ \forall\ k$ (see figure 6). Thus, the memory can also tolerate small site-to-site variations ($\sim \pm 10\%$) in the coupling strengths θ_k.

5. Implementation

Having established the operation and robustness of the quantum memory chain, we now turn to describing it might be implemented in a first experiment. We choose as a platform *bosonic* ultracold atoms in optical dipole-trap arrays [15–21], with one atom per site [22–24]. A spatial light modulator (SLM) can be used to generate the required trapping potential by imaging the correct pattern onto the atoms in two dimensions and having a light sheet in the other dimension to confine all atoms to a single plane [24]. The memory is in the *Mott* insulator regime, while the SLM can dynamically reconfigure the potential rapidly to ballistically transport each 'flying' atom in a controlled, deterministic fashion [24]. The two-channel system Hamiltonian can be written as

$$H = \sum_{i,\sigma}\left[\xi_a n_{i\sigma} + U n_{i\sigma} n_{i\bar{\sigma}} + \frac{V}{2} n_{i\sigma}\left(n_{i\sigma} - 1\right)\right] + \sum_{k,\sigma} \xi_k n_{k\sigma} + \sum_{i,k,\sigma}\left(\mathsf{T}_{ki} c_{k\sigma}^{\dagger} a_{i\sigma} + \mathsf{T}_{ki}^{*} a_{i\sigma}^{\dagger} c_{k\sigma}\right), \quad (18)$$

where $c_{k\sigma}^{\dagger}$ ($c_{k\sigma}$) is the bosonic, (flying) conduction-channel creation (annihilation) operator in k-space, $a_{i\sigma}^{\dagger}$ ($a_{i\sigma}$) is the bosonic, (static) valence-channel creation (annihilation) operator at site i, with $n_{k\sigma} = c_{k\sigma}^{\dagger} c_{k\sigma}$ and $n_{i\sigma} = a_{i\sigma}^{\dagger} a_{i\sigma}$; here, the index σ labels two relevant internal states of each atom, and can be treated as the effective spin ($\uparrow$, $\downarrow$). Hopping between the widely spaced Mott atoms is neglected, while we have a spin-independent tunnelling term T_{ki} between the two channels, allowing SLM-controlled exchange interaction between the flying atom and the relevant static one. As the atoms are bosonic, on-site Coulomb repulsion in the valence channel include terms between opposite spins (U) as well as parallel ones (V), while those for the conduction channel are ignored since only one flying atom is present at any time [27, 28].

Equation (18) is the bosonic periodic *Anderson* model, which gives the (bosonic) *s-d* Hamiltonian upon second-order perturbation expansion, transforming to the effective *XXZ* exchange Hamiltonian

$$H_k^{\text{eff}} = \sum_{\mu} J_{k\mu} \sigma_{\mu}^{f} \sigma_{\mu}^{s_k}, \qquad \mu \in \{x, y, z\}. \tag{19}$$

The transformation is derived in detail in appendix E [27, 28], where we also state the relationship of the $J_{k\mu}$ on tunnelling and Coulomb energies. This relationship demonstrates that the ratio J_z/J_x can be tuned to arbitrary values by changing the intensity, frequency, and polarization of the trapping light [28].

We can thus use the SLM to release and transport one atomic qubit at a time (see figure 1) [24], and control the potential such that its subsequent sequential interaction with each static spin is of the XY type by appropriate choice of model parameters [28]. A typical exchange coupling can be obtained from the experiments in [25] and is in the range 0.1–10 kHz; a typical decoherence time for atoms in optical lattice is around 1 s [26]; these are in a very promising ratio that would enable our idea to be implemented.

6. Conclusion

We have proposed a collective atomic quantum memory to store the quantum state of atoms, which is distinct from earlier work showing the mapping of single photons onto an atomic ensemble [5, 6]. The memory is resilient to various imperfections and can smooth the statistical fluctuations in local information loss. Neither the encoding nor the decoding operations requires active quantum control, and moreover the scheme can work with arbitrary coupling strengths: both offer advantages for experimental realization. Our scheme is not limited to cold atoms, and could be exploited in any architecture where the XY exchange model may be realized.

Acknowledgements

The authors are grateful to Kai Bongs for useful discussions. BWL acknowledges the Royal Society for a University Research Fellowship. YP thanks Hertford College, Oxford for support from their scholarship program.

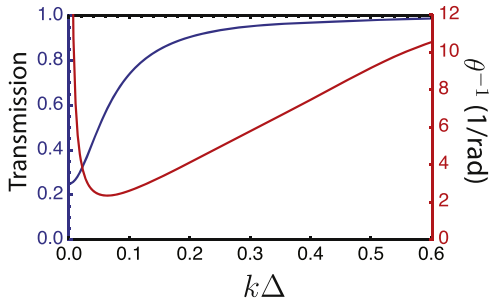

Figure A1. Transmission probability of a flying spin incident on a tight-binding chain, Anderson coupled to a single site, as a function of incident wave vector k. Also shown is the inverse of the interaction angle θ (compare to equation (2) of the main text). The spacing of sites in the chain is Δ, other parameters are $U/t = V/2t = 15$, with t the tunnel coupling of the tight binding chain and the coupling of the chain to the extra site. All single particle site energies are set equal to zero.

Appendix A. Validity of time dependent Hamiltonian

In equation (1) of the main text we use a time dependent g_k^i to model the interaction between the static and flying spins. We assert that we can assume the coupling is time dependent since the flying spin is moving, and the exchange coupling will depend on the separation of the two spins.

We have explicitly checked that the time dependent form is valid by taking a static model in which a linear, tight-binding, chain of tunnel-coupled sites carries the flying qubit. An additional single static spin is then assumed to be tunnel coupled to the middle site of the chain, through an Anderson-type Hamiltonian, which allows for double occupation of the static site but not double occupation of the chain. The dynamics results from initializing the flying particle into a travelling wave state at one end of the chain, characterized by a wave vector k. We then solve the scattering problem and calculate the transmission amplitude and probability of the flying spin as it passes the static spin. As displayed in figure A1, as k increases, the energy of the incident particle becomes larger than the effective barrier presented by the coupling to the static spin site, and the transmission probability approaches unity. In this regime, we can use the phase shifts on each spin combination to calculate the effective spin unitary operation that occurs between the static spin and the transmitted flying spin emerging from the chain. We can compare this with the ideal unitary gate of equation (2) of the main paper and extract the characteristic angle θ_k^i that appears in that equation.

We plot the result in figure A1. We see that at high transmission $\theta_k^i \equiv \theta$ is inversely proportional to k. This is in agreement with our time-dependent model: the velocity of the flying spin is proportional to k and so we expect the interaction time (and so θ) to be inversely proportional to k.

Appendix B. Collective one-spin down-flip distributions

In the main text, we introduced the lth collective one-spin down-flip distribution $D_l^{(1)} = \sum_k a_l^{(1)}(k)\sigma_k^-$ in equations (13)–(15); $|a_l^{(1)}(k)|^2$ corresponds to the probability of the kth static spin being $|\downarrow\rangle_{s_k}$ in the respective distribution.

Arising from the chain state after encoding the first flying $|\downarrow\rangle_{f_1}$ qubit (see equation (3) in the main text), the 0th one-spin down-flip distribution has $a_0^{(1)}(k) = -\mathrm{i}\sin\theta\cos^{k-1}\theta$. The total probability is $\sum_{k=1}^{\infty}|a_0^{(1)}(k)|^2 = 1$, while the mean position $\mu_0^{(1)}$ of the down-flip and the associated standard deviation $\sigma_0^{(1)}$ are (see appendix F)

$$\mu_0^{(1)} = \sum_{k=1}^{\infty} k\left|a_0^{(1)}(k)\right|^2 = \csc^2\theta,$$
$$\sigma_0^{(1)} = \sqrt{\sum_{k=1}^{\infty} k^2\left|a_0^{(1)}(k)\right|^2 - \left(\mu_0^{(1)}\right)^2} = \cos\theta\csc^2\theta. \tag{B.1}$$

The lth collective one-spin down-flip distribution in the memory results from further encoding l subsequent flying $|\uparrow\rangle_f$ qubits. We now inductively derive the analytical expression for $a_l^{(1)}(k)$ given by equation (15) in the main text. First, we find that after encoding one flying $|\uparrow\rangle_f$ qubit into a chain with state $\sigma_k^-|F\rangle_c$ $\forall$ finite $k \ll N$, the total state becomes

$$|\uparrow\rangle_f \otimes \left(\cos\theta\,\sigma_k^- - \sin^2\theta\sum_{n=k+1}^{\infty}\cos^{n-k-1}\theta\,\sigma_n^-\right)|F\rangle_c, \tag{B.2}$$

which is derived step-by-step as before. Thus, by linearity (apply equation (B.2)), encoding one flying $|\uparrow\rangle_f$ qubit into the chain with distribution $D_0^{(1)} = \sum_k a_0^{(1)}(k)\sigma_k^-$ gives rise to the first one-spin down-flip distribution

$$D_1^{(1)} = \sum_{k=1}^{\infty} a_0^{(1)}(k)\left(\cos\theta\,\sigma_k^- - \sin^2\theta\sum_{n=k+1}^{\infty}\cos^{n-k-1}\theta\,\sigma_n^-\right). \tag{B.3}$$

Again, we want to focus on the coefficients of σ_k^- terms for the double sum. Note that $a_0^{(1)}(k)/\cos^{k-1}\theta = -\mathrm{i}\sin\theta$, independent of k. Thus, the double sum in equation (B.3) is

$$\begin{aligned}
&-\sin^2\theta\sum_{k=1}^{\infty}\sum_{n=k+1}^{\infty} a_0^{(1)}(k)\cos^{n-k-1}\theta\,\sigma_n^- \\
&= -\tan^2\theta\sum_{k=1}^{\infty}\sum_{n=k+1}^{\infty}(-\mathrm{i}\sin\theta)\cos^n\theta\,\sigma_n^- \\
&= -\tan^2\theta(-\mathrm{i}\sin\theta)\sum_{n=1}^{\infty}\sum_{k=n+1}^{\infty}\cos^k\theta\,\sigma_k^- \\
&= -\tan^2\theta(-\mathrm{i}\sin\theta)\sum_{k=1}^{\infty}(k-1)\cos^k\theta\,\sigma_k^- \\
&= -\tan^2\theta\sum_{k=1}^{\infty}(k-1)\,a_0^{(1)}(k)\cos\theta\,\sigma_k^-,
\end{aligned} \tag{B.4}$$

where we have interchanged the labelling of dummy variables n and k in the third line, and evaluated the sum of geometric series in the fourth. Substituting this back into equation (B.3) (and compare with the more general definition of $D_l^{(1)}$), we have

$$a_1^{(1)}(k) = a_0^{(1)}(k)\cos\theta\Big(1-(k-1)\tan^2\theta\Big). \tag{B.5}$$

We can then apply the same procedure (with equation (B.2) to encoding one flying $|\uparrow\rangle_f$ qubit into $D_1^{(1)} = \sum_k a_1^{(1)}(k)\sigma_k^-$ to find, again by linearity, amplitudes for the second one-spin down-flip distribution

$$a_2^{(1)}(k) = a_0^{(1)}(k)\cos^2\theta\Big(1-2(k-1)\tan^2\theta+\frac{(k-1)(k-2)}{2}\tan^4\theta\Big), \tag{B.6}$$

where (as also illustrated in equation (B.4) we have evaluated the following weighted sums of geometric series (by first relabelling the dummy variables to focus on σ_k^-)

$$\begin{aligned}\sum_{k=1}^{\infty}\sum_{n=k+1}^{\infty}(k-1)\cos^n\theta\,\sigma_n^- &= \sum_{n=1}^{\infty}\sum_{k=n+1}^{\infty}(n-1)\cos^k\theta\,\sigma_k^- \\ &= \sum_{k=2}^{\infty}\Big(\sum_{n=1}^{k-1}(n-1)\Big)\cos^k\theta\,\sigma_k^- \\ &= \sum_{k=3}^{\infty}\frac{(k-1)(k-2)}{2}\cos^k\theta\,\sigma_k^-.\end{aligned} \tag{B.7}$$

Note that the general term of the bracketed series in the second line are obtained from evaluation of the weighted geometric series in the previous step (from evaluating the lower order distribution).

Now, with the key inductive steps to relabel the dummy variables (to focus on σ_k^-), and to evaluate the following series (as done above and in equation (B.4))

$$\sum_{n=l'+1}^{k-1}\frac{(-1)^{l'}}{l'!}\prod_{m=0}^{l'-1}\frac{(l'-m)}{l'!}\prod_{j=1}^{l'}(n-j)\equiv\frac{(-1)^{l'+1}}{(l'+1)!}\prod_{j=1}^{l'+1}(k-j), \tag{B.8}$$

we can inductively derive

$$\begin{aligned}a_l^{(1)}(k) &= a_0^{(1)}(k)\cos^l\theta\times\sum_{r=0}^{\min\{l,k-1\}}(-1)^r\Big(\frac{1}{r!}\prod_{m=0}^{r-1}(l-m)\Big)\frac{1}{r!}\prod_{j=1}^{r}(k-j)\tan^{2r}\theta \\ &= a_0^{(1)}(k)\cos^l\theta\sum_{r=0}^{\min\{l,k-1\}}(-1)^r\binom{k-1}{r}\binom{l}{r}\tan^{2r}\theta \\ &= a_0^{(1)}(k)\cos^l\theta\,{}_2F_1\Big(1-k,-l;1;-\tan^2\theta\Big).\end{aligned} \tag{B.9}$$

Note that equation (B.2) has two terms, the first (and lower order) of which inductively adds to the lower order terms (in $\tan^2\theta$) in equation (B.9), to give rise to the bracketed product coefficient concerning l. □

In the more compact form of equation (B.9), ${}_2F_1(a,b;c;z)$ denotes the *Gauss* hypergeometric function [14], and $a_0^{(1)}(k)\cos^l\theta$ renders possible divergence of $\tan^{2r}\theta$ convergent in equation (B.9) (analytic continuation is assumed implicitly here). This expression for the lth collective one-spin down-flip distribution can also be obtained through a combinatorial argument, as follows. For any fixed down-flip position k, and assuming $k > (l+1)$, the amplitude is a sum of $l+1$ terms, each of which corresponds to a different

origin for the σ_k^-. In general a spin-up qubit passing along the chain can either cause no spin flips at all, or can move a spin down from a site nearer the front of the chain to one further along it. The 0th term results from the situation in which the down spin is initially localized on spin state k and where all l subsequent $|\uparrow\rangle_f$ qubits move along the chain without executing further flips. Each has contributed a factor of $\cos\theta$ due to the exchange interaction and thus an overall factor of $\cos^l\theta$ is present in addition to $a_0^{(1)}(k)$. In general, the rth term ($r > 0$) occurs when r movements of the initial spin down position occur before that spin down reaches its final position k. There are $\binom{l}{r}$ ways of choosing the r qubits which cause the flips from the l total, and $\binom{k-1}{r}$ ways of choosing which r of the $(k-1)$ static spins which precede the kth will hold the spin down at some point before the spin down finally occurs at site k. The other terms in the summation come from the fact that each double spin flip (or movement of the spin down location) gives rise to a factor of $(-\mathrm{i}\sin\theta)^2$, while losing a factor of $\cos\theta$; in addition, the other $(l-r)$ $|\uparrow\rangle_f$ qubits passed the down-flipped spin without exchanging, and each contributed a factor of $\cos\theta$. Combining these coefficients gives rise to equation (B.9).

Decoding this more general memory state can be achieved by injecting successive $|\uparrow\rangle_f$ spins in the decoding direction. After the first such spin passes, the new memory state down-spin amplitude for the kth site, $a'^{(1)}_{l-1}(k)$, results from two possible scenarios: either this $|\uparrow\rangle_f$ passed the kth site which was already in the down state, without exchange, or it transported the $(k+s)$th down spin to the kth position. Taking into account of the factors contributed, we have

$$\begin{aligned} a'^{(1)}_{l-1}(k) &= a_l^{(1)}(k)\cos\theta + (-\mathrm{i}\sin\theta)^2\sum_{s=1}^{\infty} a_l^{(1)}(k+s)\cos^{s-1}\theta \\ &\equiv a^{(1)}_{l-1}(k). \end{aligned} \tag{B.10}$$

To establish this last equivalence, we multiply both sides of the following identity (see appendix G)

$$\frac{{}_2F_1(a,b;1;z)}{1-z} + \frac{z}{1-z}\sum_{s=1}^{\infty}\frac{{}_2F_1(a-s,b;1;z)}{(1-z)^s} \equiv {}_2F_1(a,b+1;1;z) \tag{B.11}$$

by $a_0^{(1)}(k)\cos^{l-1}\theta$, and substitute for $a = 1-k$, $b = -l$, and $z = -\tan^2\theta$; we then obtain $a'^{(1)}_{l-1}(k) \equiv a^{(1)}_{l-1}(k)$ from equation (B.10). Here, $l \in \mathbb{N}$ can be arbitrary. This means that the one-spin down-flip distributions can be manipulated in both directions, essential for the chain to act as a memory.

Having established this important feature, we now show that each distribution corresponds to a unique storage mode and the modes are independent, i.e., expressed as the following (discrete) orthonormal condition

$$\sum_{k=1}^{\infty} a_{l'}^{(1)*}(k)\, a_l^{(1)}(k) = \delta_{l'l}. \tag{B.12}$$

This ensures the unit total probability for each distribution. To establish this discrete orthonormal condition equation (B.12), we first introduce the normalized *Meixner* polynomials [14] (with j, x integers)

$$M'_j(x;\,\mu,\,\nu):\;=\;\nu^{\frac{j}{2}}\;{}_2F_1\left(-j,\,-x;\,\mu;\,1-\frac{1}{\nu}\right)\equiv\;\nu^{\frac{j}{2}}\;{}_2F_1\left(-x,\,-j;\,\mu;\,1-\frac{1}{\nu}\right), \tag{B.13}$$

where the equivalence comes from the symmetry of the hypergeometric function in its first two arguments. Note that the different normalization is present since we are only summing over $x \in \mathbb{N}$ (instead of $\mathbb{Z}$). The orthonormality condition for the Meixner polynomials states

$$\sum_{x=0}^{\infty} M'_j(x;\,\mu,\,\nu)M'_{j'}(x;\,\mu,\,\nu)\omega(x;\,\mu,\,\nu)=\delta_{jj'}, \tag{B.14}$$

where the discrete weight $\omega(x;\,\mu,\,\nu)=(1-\nu)^{\mu}\frac{(\mu)_x}{x!}\nu^x$ [14]. Setting $x=k-1$, $j=l$, $\mu=1$, $\nu=\cos^2\theta$, and substituting equation (B.13) into equation (B.14), we have

$$\sum_{k=1}^{\infty}\;{}_2F_1\left(1-k,\,-l;\,1;\,-\tan^2\theta\right)\;{}_2F_1\left(1-k,\,-l';\,1;\,-\tan^2\theta\right)\sin^2\theta\,\cos^{2(k+l-1)}\theta$$
$$=\delta_{ll'}, \tag{B.15}$$

which is exactly the desired condition equation (B.12). Note that one special case of the Meixner polynomials are the *Krawtchouk* polynomials [14], which have recently been applied to works involving QST of a single spin excitation within certain linear, interacting spin chains [29].

The independence of these unique storage modes are best illustrated by considering their mean positions $\mu_l^{(1)}$ of the down-flip and the corresponding standard deviations $\sigma_l^{(1)}$, which can be calculated in a similar way to how we found equation (B.1). We find that for any given coupling strength θ, both $\mu_l^{(1)}$ and $\sigma_l^{(1)}$ increase *linearly* with l; an example is demonstrated in figure B1 , with a non-special value $\theta=0.4$, say.

Finally, we numerically simulate (see also appendix H) the down-flip distributions, by encoding a flying $|\downarrow\rangle_f$ qubit followed by l subsequent $|\uparrow\rangle_f$ into the initially ferromagnetically polarized chain. An example is shown in figure B2 , and shows agreement with our analytical solutions for $|a_l^{(1)}(k)|^2$.

Appendix C. (0, 0)th two-spin down-flip distribution

To generalize the results, we need to show that the chain can store a spin state that includes an arbitrary number n of down-spins

$$D^{(n)}_{(l_1,\ldots,l_n)}=\sum_{k_1<\ldots<k_n} a^{(n)}_{(l_1,\ldots,l_n)}(k_1,\ldots,k_n)\;\sigma^{-}_{(k_1,\ldots,k_n)}, \tag{C.1}$$

where the k_is denote the spin–flip positions and l_i denotes the number of $|\uparrow\rangle_f$ encoded between the ith and $(i+1)$th flying $|\downarrow\rangle_f$ qubits. This would mean that the chain can store the information from a number of flying qubits, each of which was originally either $|\uparrow\rangle_f$ or $|\downarrow\rangle_f$ and can be further retrieved by the aforementioned decoding mechanism. By linearity, it could also store any superposition, which would confirm its status as a true quantum memory. We, however, are unable to prove the general case due to the increasing complexity of the analytical solution (with large numbers of parameters l_is and k_js). Here, we derive the analytical expression for the (0, 0)th collective two-spin down-flip distribution

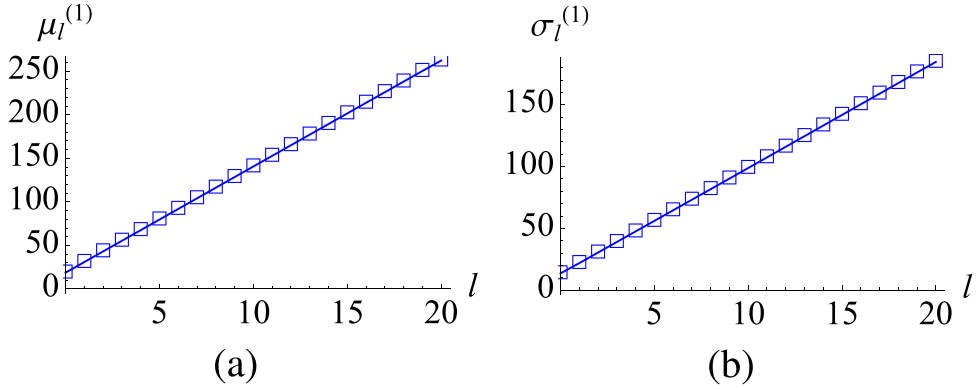

Figure B1. Plots with a non-special coupling strength $\theta = 0.4$ for (a) the mean positions $\mu_l^{(1)}$ of the down-flip against the number l of subsequent flying $|\uparrow\rangle_f$ qubits encoded into the memory; (b) the corresponding standard deviations $\sigma_l^{(1)}$ against l. The linear relationships are also observed for other θ values.

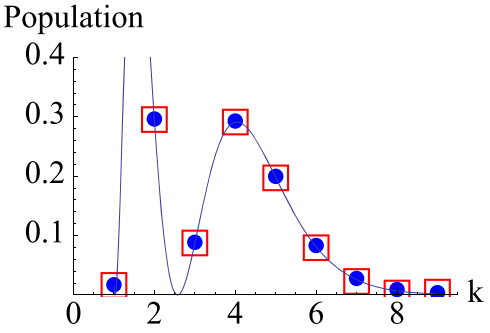

Figure B2. Plots of the down-flip distribution $|a_2^{(1)}(k)|^2$ in a chain with $N = 9$, and $\theta = 1.2$: The discrete plots are from our simulations ('blue circle' for $|a_2^{(1)}(k)|^2$ and 'red square' for $|a'^{(1)}_2(k)|^2$), while the curve corresponds to the analytical solution equation (B.9) (only values for integer k are relevant).

$$D^{(2)}_{(0,\,0)} = \sum_{k_1<k_2} a^{(2)}_{(0,\,0)}(k_1,\,k_2)\;\sigma^{-}_{(k_1,\,k_2)}, \tag{C.2}$$

after having encoded only two $|\downarrow\rangle_f$ in the chain. Going through step-by-step we find that the total state of the system, after encoding one flying $|\downarrow\rangle_f$ qubit into a chain with state $\sigma_k^-|F\rangle_c$, becomes

$$|\uparrow\rangle_f \otimes (-\mathrm{i}\,\sin\theta)\sum_{k'=2}^{\infty}\cos^{k'-2}\theta\sigma_k^-\sigma_{k'}^-|F\rangle_c \quad \text{if } k=1, \tag{C.3}$$

or $\forall$ finite $2 \leqslant k \ll N$

$$|\uparrow\rangle_f \otimes (-\mathrm{i}\,\sin\theta) \times\left[\sum_{k'=k+1}^{\infty}\cos^{k'-2}\theta\sigma_k^-\sigma_{k'}^- + \sum_{k'=1}^{k-1}\cos^{k'}\theta\;\sigma_k^-\sigma_{k'}^-\right.$$

$$- \tan^2\theta \sum_{k'=1}^{k-1}\sum_{k''=k+1}^{\infty} \cos^{k'+k''-k}\theta\sigma_{k'}^{-}\sigma_{k''}^{-}\Bigg]|F\rangle_c. \tag{C.4}$$

Note that by applying a combinatorial argument as illustrated before, one can obtain the same results.

Thus by linearity, after encoding the $|\downarrow\rangle_f$ into $D_0^{(1)}|F\rangle_c$, we have

$$D_{(0,\,0)}^{(2)} = (-\mathrm{i}\sin\theta)^2\Bigg[\sum_{k=1}^{\infty}\sum_{k'=k+1}^{\infty}\cos^{k+k'-3}\theta\;\sigma_k^{-}\sigma_{k'}^{-} + \sum_{k=2}^{\infty}\Bigg(\sum_{k'=1}^{k-1}\cos^{k+k'-1}\theta\;\sigma_k^{-}\sigma_{k'}^{-} - \tan^2\theta\sum_{k'=1}^{k-1}\sum_{k''=k+1}^{\infty}\cos^{k'+k''-1}\theta\sigma_{k'}^{-}\sigma_{k''}^{-}\Bigg)\Bigg]. \tag{C.5}$$

By manipulating the double and triple summations as before, we find that

$$D_{(0,\,0)}^{(2)} = (-\mathrm{i}\sin\theta)^2\sum_{k_1=1}^{\infty}\sum_{k_2=k_1+1}^{\infty}\Big(\cos^{k_1+k_2-3}\theta + \cos^{k_1+k_2-1}\theta - \big(k_2-k_1-1\big)\tan^2\theta\,\cos^{k_1+k_2-1}\theta\Big)\sigma_{k_1}^{-}\sigma_{k_2}^{-}. \tag{C.6}$$

Therefore, the (0, 0)th collective two-spin amplitude is

$$a_{(0,\,0)}^{(2)}\big(k_1,\,k_2\big) = (-\mathrm{i}\sin\theta)^2\cos^{k_1+k_2-1}\theta\times\Big(2-\big(k_2-k_1-2\big)\tan^2\theta\Big), \tag{C.7}$$

as quoted in the main text. We have the total probability $\sum_{k_1<k_2}|a_{(0,0)}^{(2)}(k_1,\,k_2)|^2 = 1$. The qubits can also be recovered sequentially, as can be shown by going through step-by-step or using a combinatorial argument.

We have thus shown that the memory can encode and decode $|\uparrow_{f_2}\;\uparrow_{f_1}\rangle$, $|\uparrow_{f_2}\;\downarrow_{f_1}\rangle$, $|\downarrow_{f_2}\;\uparrow_{f_1}\rangle$, and $|\downarrow_{f_2}\;\downarrow_{f_1}\rangle$; by linearity, the memory can store two qubits of arbitrary state, *entangled* or not (and hence qubits of mixed states). We conjecture that the memory chain can store multiple flying qubits of arbitrary states using the described mechanism (see an example of numerical simulations of larger memory states from figure 5 in the main text supporting this conjecture).

Appendix D. Special case for multiple qubits

In this appendix we consider the special case $\theta = \pi/2$ and derive explicit expressions for the quantum state storage and retrieval of n initial flying qubits in an arbitrary superposition state incident on a chain of $N > n$ spins that are, as usual, ferromagnetically aligned and do not interact with each other. We see from equation (2) in the main text that for $\theta = \pi/2$ there is an exchange of flying and static spins for forward scattering, i.e.

$$\left|\uparrow^f\;\uparrow^s\right\rangle \rightarrow \left|\uparrow^s\;\uparrow^f\right\rangle \tag{D.1}$$

$$\left|\uparrow^f\;\downarrow^s\right\rangle \rightarrow (-i)\left|\uparrow^s\;\downarrow^f\right\rangle \tag{D.2}$$

$$\left| \downarrow^f \uparrow^s \right\rangle \rightarrow (-i) \left| \downarrow^s \uparrow^f \right\rangle \tag{D.3}$$

$$\left| \downarrow^f \downarrow^s \right\rangle \rightarrow \left| \downarrow^s \downarrow^f \right\rangle, \tag{D.4}$$

where we have shown explicitly the position of the flying qubit relative to the static qubit. This is essentially a SWAP operation with extra factor $(-i)$ when the spins are antiparallel and undergo spin flips. Consider an initial state with n flying qubit spins with each spin orientation either up or down, i.e.

$$\left| \sigma_n^f \sigma_{n-1}^f \ldots \sigma_1^f F_N^s \right\rangle, \tag{D.5}$$

where

$$\left| F_N^s \right\rangle = \left| \uparrow_1^s \ \uparrow_2^s \ \ldots \ \uparrow_N^s \right\rangle. \tag{D.6}$$

After all flying qubits have been transmitted, emerging as up-spins, we get

$$\left| \sigma_n^f \sigma_{n-1}^f \ldots \sigma_1^f F_N^s \right\rangle \rightarrow z_{\sigma_1 \ldots \sigma_n} \left| \sigma_n^s \sigma_{n-1}^s \ldots \sigma_1^s F_{N-n}^s F_n^f \right\rangle, \tag{D.7}$$

where $z_{\sigma_1 \ldots \sigma_n} = (-i)^{2p} = \pm 1$ for an even number of down-spins and $z_{\sigma_1 \ldots \sigma_n} = (-i)^{2p+1} = \pm i$ for an odd number of down-spins ($p = 0, 1, 2, \ldots$). This follows from the fact that there must be an even number of spin flips when when there is an even number (or zero) down-spins in the initial state and an odd number of spin flips when there is an odd number of down-spins in the initial state. The integer p depends on the specific distribution of up-spins and down-spins in the initial state but is not needed explicitly for our purposes. The relation equation (D.7) is proved by induction. Assuming it is true for n then

$$\begin{aligned} \left| \sigma_{n+1}^f \sigma_n^f \ldots \sigma_1^f F_N^s \right\rangle &\rightarrow z_{\sigma_1 \ldots \sigma_n} \left| \sigma_{n+1}^f \sigma_n^s \sigma_{n-1}^s \ldots \sigma_1^s F_{N-n}^s F_n^f \right\rangle \\ &\rightarrow (-i)^{n_{sf}} z_{\sigma_1 \ldots \sigma_n} \left| \sigma_{n+1}^s \sigma_n^s \ldots \sigma_1^s F_{N-n-1}^s F_{n+1}^f \right\rangle, \end{aligned} \tag{D.8}$$

where n_{sf} is the number of spin flips encountered when the $(n+1)$ th flying qubit is transmitted through the chain and must be an even integer (or zero) if σ_{n+1} is up and an odd integer if σ_{n+1} is down. Hence we may write the final state as

$$z_{\sigma_1 \ldots \sigma_{n+1}} \left| \sigma_{n+1}^s \sigma_n^s \ldots \sigma_1^s F_{N-n-1}^s F_{n+1}^f \right\rangle, \tag{D.9}$$

where $z_{\sigma_1 \ldots \sigma_{n+1}}$ has the same meaning as before. Hence, if equation (D.7) is true for n it is also true for $n+1$ and hence for all n since it is certainly true for $n = 1$. In a similar fashion we may show that for the read operation

$$z_{\sigma_1 \ldots \sigma_n} \left| \sigma_n^s \sigma_{n-1}^s \ldots \sigma_1^s F_{N-n}^s F_n^f \right\rangle \rightarrow z_{\sigma_1 \ldots \sigma_n}^2 \left| \sigma_n^f \sigma_{n-1}^f \ldots \sigma_1^f F_N^s \right\rangle, \tag{D.10}$$

i.e. we recover the original flying qubits state for an even number of down-spins for which $z_{\sigma_1 \ldots \sigma_n}^2 = 1$. For an odd number of down-spins there is thus a sign change of the state since $z_{\sigma_1 \ldots \sigma_n}^2 = -1$.

For a general superposition state, i.e. an initial state

$$\sum_{\sigma_1 .. \sigma_n} \alpha_{\sigma_1 .. \sigma_n} \left| \sigma_n^f \sigma_{n-1}^f \ldots \sigma_1^f F_N^s \right\rangle, \tag{D.11}$$

the state after propagation of all flying qubits becomes

$$\sum_{\sigma_1..\sigma_n} \alpha_{\sigma_1..\sigma_n} z_{\sigma_1..\sigma_n} \left|\sigma_n^s \sigma_{n-1}^s ... \sigma_1^s F_{N-n}^s F_n^f\right\rangle. \tag{D.12}$$

Thus the original superposition state is not, in general, transferred to the static qubits. For example, the states of the two incident qubits in the spin singlet state is transferred to the first two static qubits as an $S_z = 0$ spin triplet, i.e.

$$\begin{aligned}\left(\left|\uparrow^f \downarrow^f\right\rangle - \left|\downarrow^f \uparrow^f\right\rangle\right) \otimes \left|F_N^s\right\rangle &\rightarrow i\left(\left|\uparrow^s \downarrow^s\right\rangle + \left|\downarrow^s \uparrow^s\right\rangle\right) \otimes \left|F_{N-2} F_2^f\right\rangle \\ &\rightarrow -\left(\left|\uparrow^f \downarrow^f\right\rangle - \left|\downarrow^f \uparrow^f\right\rangle\right) \otimes \left|F_N^s\right\rangle \end{aligned} \tag{D.13}$$

but restored to the singlet after the read operation, apart from an unimportant overall sign change. This result is readily extended to general superposition states for which all components have either an even number of down-spins or an odd number of down-spins, thus recovering the initial state after a write-read cycle with a sign change for an odd number of down spins. Whilst this sign change is unimportant for these cases it is important for states with admixtures of base states containing both even and odd numbers of down-spins. A simple example is the single-flying qubit case discussed in sections 2.1 and 2.2, giving the write-read cycle

$$\begin{aligned}\left(\alpha\left|\uparrow^f\right\rangle + \beta\left|\downarrow^f\right\rangle\right) \otimes \left|F_N^s\right\rangle &\rightarrow \left(\alpha\left|\uparrow^s\right\rangle - \mathrm{i}\beta\left|\downarrow^s\right\rangle\right) \otimes \left|F_{N-1} F_1^f\right\rangle \\ &\rightarrow \left(\alpha\left|\uparrow^f\right\rangle - \beta\left|\downarrow^f\right\rangle\right) \otimes \left|F_N^s\right\rangle \\ &\underset{\rightarrow}{\sigma_z} \left(\alpha\left|\uparrow^f\right\rangle + \beta\left|\downarrow^f\right\rangle\right) \otimes \left|F_N^s\right\rangle, \end{aligned} \tag{D.14}$$

where in the last step the correct sign for the down-spin component is restored with a σ_z gate. This is readily generalized to any arbitrary superposition where a final σ_z gate applied to all flying qubits will restore the correct sign to all components with an odd number of down spins.

Appendix E. Bosonic periodic Anderson model

In the main text, we described an implementation of the memory system with a two-channel bosonic atom lattice, to be controlled by a SLM; here we describe how we arrived at the effective spin Hamiltonian describing this situation.

Consider first the case of a single site in the localized channel containing a bound-state atom and a single atom injected into the propagating channel. Neglecting interactions between atoms in the propagating channel, we may describe this system by the single-site bosonic *Anderson* model [27]

$$H = \sum_k \xi_k n_k + \xi_a n + U n_\uparrow n_\downarrow + \frac{1}{2} V \sum_\sigma n_\sigma (n_\sigma - 1) + \sum_\sigma \left(\mathsf{T}_k c_{k\sigma}^\dagger a_\sigma + \mathsf{T}_k^* a_\sigma^\dagger c_{k\sigma}\right), \tag{E.1}$$

where U is the repulsion energy between atoms in the same localized 'orbital' state but opposite effective spin whereas V is that for the same effective spin; $n_k = c_{k\uparrow}^\dagger c_{k\uparrow} + c_{k\downarrow}^\dagger c_{k\downarrow}$ and $n = a_\uparrow^\dagger a_\uparrow + a_\downarrow^\dagger a_\downarrow$ (with notations adapted from the main text).

We are interested in the regime for which $\xi_a < \xi_k < \xi_a + \min\{U, V\}$, in which case the Anderson model may be transformed into the so-called *s-d* model by second-order perturbation

theory. The base states with two atoms in either the localized channel or the propagation channel become intermediate states, and are thus eliminated from the problem. If we choose the kinetic energy of the propagating atom to be sufficiently large, then backscattering is negligible and there is in general a spin exchange between the static atom and the propagating atom described by the effective Hamiltonian

$$H^{\text{eff}} = \sum_{k,\,k'} \left[J^{x,y}_{k\,k'} \left(S^{+} c^{\dagger R}_{k\downarrow} c^{L}_{k'\uparrow} + S^{-} c^{\dagger R}_{k\uparrow} c^{L}_{k'\downarrow} \right) + J^{z}_{k\,k'} S^{z} \left(c^{\dagger R}_{k\uparrow} c^{L}_{k'\uparrow} - c^{\dagger R}_{k\downarrow} c^{L}_{k'\downarrow} \right) \right], \tag{E.2}$$

where

$$J^{x,y}_{k\,k'} = \mathsf{T}^{*}_{k} \mathsf{T}_{k'} \left[\frac{1}{U - (\xi_k - \xi_a)} + \frac{1}{\xi_k - \xi_a} \right],$$

$$J^{z}_{k\,k'} = J^{x,y}_{k\,k'} - \frac{2\left|\mathsf{T}_k\right|^2 \delta_{k\,k'}}{V - (\xi_k - \xi_a)},$$

and we have introduced explicitly the superscripts L and R to emphasize destruction and creation of forward propagating electrons to the left and right of the localized site; S^z and $S^{\pm} = S^x \pm \mathrm{i}S^y$ are the spin operators.

Equation (E.2) is the usual *s-d* Hamiltonian for fermions [27], apart from the extra (bosonic) term in $J^z_{k\,k'}$, which reduces $J^z_{k\,k'}$. By tuning the energy parameters ξ_a, ξ_k, T_k, U and V, we can choose $J^z_{k\,k'} = 0$ (when $U = V = 2(\xi_k - \xi_a)$ in the forward scattering regime $k = k'$) resulting in the XY model.

In order to determine the change in spin states of the localized and propagating atoms explicitly we have, of course, to solve the scattering problem for H^{eff} in equation (E.2). In the main text, this was discussed within the framework of time-dependent evolution of a spin model (XY) for which the exchange parameters vary with time. This is equivalent to solving the time-independent scattering problem using the effective Hamiltonian in equation (E.2) as may be shown explicitly by either forming a wavepacket for the initial state or by comparing directly the time dependent method using equation (1) in the main text (for a single localized qubit and the single flying qubit) and the time-independent scattering solution using equation (E.2).

The method described above for a single propagating atom and single localized atom is readily generalized to multiple localized sites, each populated with a single atom, and sequential injection of propagating atoms. This is the two-channel periodic Anderson model for bosonic atoms, equation (18) in the main text, for which we choose the localized (periodic) sites to be sufficiently separated to form a *Mott* insulating chain with negligible direct interaction between neighbours. Thus all interactions between propagating and localized atoms take place through the independent binary scattering processes described above.

Appendix F. Mathematical identity I

Calculations of the mean and standard deviation in equation (B.1) involves evaluating series of the following forms

$$\sum_{k=1}^{\infty} k y^{k-1} \equiv \frac{\mathrm{d}}{\mathrm{d}y}\left(\sum_{k=1}^{\infty} y^k\right) = \frac{\mathrm{d}}{\mathrm{d}y}\left(\frac{y}{1-y}\right) = \frac{1}{(1-y)^2}, \tag{F.1}$$

$$\begin{aligned}\sum_{k=1}^{\infty} k^2 y^{k-1} &\equiv \sum_{k=1}^{\infty}(k+1)k y^{k-1} - \sum_{k=1}^{\infty} k y^{k-1} \\ &\equiv \frac{\mathrm{d}^2}{\mathrm{d}y^2}\left(\sum_{k=1}^{\infty} y^{k+1}\right) - \frac{1}{(1-y)^2} \\ &\equiv \frac{\mathrm{d}^2}{\mathrm{d}y^2}\left(\frac{y^2}{1-y}\right) - \frac{1}{(1-y)^2} = \frac{1+y}{(1-y)^3}.\end{aligned} \tag{F.2}$$

We then set $y = \cos^2\theta$ for the two final formulae, and substitute back into equation (B.1) for evalutions.

Appendix G. Mathematical identity II

In order to show that $a'^{(1)}_{l\,-\,1}$ (equation (B.10)) is the same as $a^{(1)}_{l\,-\,1}$, we applied the identity stated in equation (B.11)

$$\begin{aligned}\frac{{}_2F_1(a, b; 1; z)}{1-z} + \frac{z}{1-z}\sum_{s=1}^{\infty}\frac{{}_2F_1(a-s, b; 1; z)}{(1-z)^s} \\ \equiv {}_2F_1(a, b+1; 1; z).\end{aligned} \tag{G.1}$$

To prove this, we work with the *Euler*'s integral representation for the hypergeometric function

$${}_2F_1(a, b; 1; z) = \frac{1}{B(b, 1-b)}\int_0^1 \frac{t^{b-1}(1-t)^{-b}}{(1-zt)^a}\mathrm{d}t \tag{G.2}$$

for $|z| \leqslant 1$, and apply analytic continuation to other values of z. Here, $B(p, q) = \Gamma(p)\Gamma(q)/\Gamma(p+q)$ is the *beta* function, where $\Gamma(p+1) = p\Gamma(p)$ is the *gamma* function [14]. We see that

$$B(b, 1-b) = \frac{\Gamma(b)\Gamma(1-b)}{\Gamma(1)} = \frac{\frac{1}{b}\Gamma(b+1)(-b)\Gamma(-b)}{\Gamma(1)} = -B(b+1, -b). \tag{G.3}$$

Thus, by substituting both equations (G.2) and (G.3) back into equation (B.11) (and multiplying it both sides by $(1-z)B(b, 1-b)$), our task reduces to proving that

$$\begin{aligned}\int_0^1 \frac{t^{b-1}(1-t)^{-b}}{(1-zt)^a}\mathrm{d}t + \sum_{s=1}^{\infty}\frac{z}{(1-z)^s}\int_0^1 \frac{t^{b-1}(1-t)^{-b}}{(1-zt)^{a-s}}\mathrm{d}t \\ \equiv -(1-z)\int_0^1 \frac{t^b(1-t)^{-b-1}}{(1-zt)^a}\mathrm{d}t,\end{aligned} \tag{G.4}$$

where the extra minus sign on the right hand side comes from equation (G.3). Evaluating the summation in equation (G.4), we have

$$\sum_{s=1}^{\infty}\frac{z}{(1-z)^s}\int_0^1\frac{t^{b-1}(1-t)^{-b}}{(1-zt)^{a-s}}\mathrm{d}t=\int_0^1 z\left[\sum_{s=1}^{\infty}\left(\frac{1-zt}{1-z}\right)^s\right]\frac{t^{b-1}(1-t)^{-b}}{(1-zt)^a}\mathrm{d}t$$
$$=\int_0^1 \not{z}\left(\frac{1-zt}{\not{z}(t-1)}\right)\frac{t^{b-1}(1-t)^{-b}}{(1-zt)^a}\mathrm{d}t. \tag{G.5}$$

Hence, the left hand side of equation (G.4) is equivalent to

$$\int_0^1\left(1-\frac{1-zt}{1-t}\right)\frac{t^{b-1}(1-t)^{-b}}{(1-zt)^a}\mathrm{d}t=-(1-z)\int_0^1\frac{t}{1-t}\frac{t^{b-1}(1-t)^{-b}}{(1-zt)^a}\mathrm{d}t, \tag{G.6}$$

which is exactly the right hand side of equation (G.4). □

Appendix H. Mathematical identity III

The time evolution operator for the interaction between a flying qubit and a static spin can be expressed as in equation (2) in the main text. However, each flying qubit interacts with the static spins sequentially; in order to numerically simulate the evolution for the state of the whole system $|\psi_f, \Phi_c\rangle$, we apply the write and read operators

$$U_{\text{write}}=U_{fN}\ldots U_{f2}U_{f1}$$
$$U_{\text{read}}=U_{f1}U_{f2}\ldots U_{fN}, \tag{H.1}$$

where each $2^{N+1}\times 2^{N+1}$ time evolution matrix U_{fi} describes the interaction between the flying qubit and the ith static spin under the standard basis $\{f, s_1, s_2,\ldots, s_N\}$):

$$U_{fk}=\left(\begin{array}{cc|cc}\mathbb{1}_{2^{N-k}} & \mathbb{O}_{2^{N-k}} & & \\ & \mathbb{C}_{2^{N-k}} & \mathbb{S}_{2^{N-k}} & \\ \mathbb{O}_{2^{N-k}} & & \ddots & \ddots \\ & \ddots & & \mathbb{S}_{2^{N-k}} \\ \hline & \mathbb{S}_{2^{N-k}} & \mathbb{C}_{2^{N-k}} & \mathbb{O}_{2^{N-k}} \\ & \ddots & \ddots & \\ & \mathbb{S}_{2^{N-k}} & \mathbb{O}_{2^{N-k}} & \mathbb{1}_{2^{N-k}}\end{array}\right), \tag{H.2}$$

where $\mathbb{1}_m$ is the $m\times m$ identity matrix, $\mathbb{C}_m=\cos\theta_k\,\mathbb{1}_m$ while $\mathbb{S}_m=-\mathrm{i}\sin\theta_k\,\mathbb{1}_m$; both $\mathbb{O}_m$ and blank fields correspond to blocks of 0 s. The dots represent the *alternating* repetitive patterns (along the diagonal in the upper left and lower right blocks these are $\mathbb{1}_m, \mathbb{C}_m, \mathbb{1}_m, \mathbb{C}_m$ ...; along the diagonals in the lower left and upper right blocks these are $\mathbb{S}_m, \mathbb{O}_m, \mathbb{S}_m, \mathbb{O}_m$ ...), and there are an equal number of blocks of $\mathbb{1}_m$s, $\mathbb{C}_m$s and $\mathbb{S}_m$s. This is readily obtained by considering the exchange processes between the flying qubit and the kth static spin, regardless of the state of other spins (the alternating repetitive pattern due to spins s_1 to s_{k-1} and the size of each block due to s_{k+1} to s_N). Note that each U_{fk} is symmetric, and centrosymmetric (symmetric about the centre point and a property that is closed under matrix multiplications) [30].

When the whole system is restricted to at most one excitation (as it was in the main text for considering decoherence), the state space consisting of more than one excitations is never accessed and can thus be ignored for the purpose of simulation. In this way, the dimension

$(N + 2) \times (N + 2)$ of the density matrix (with only zero or one excitation) grows linearly with the number N of chain spins; simulations of very long chains can then be done conveniently.

References

[1] Nielsen M A and Chuang I L 2010 *Quantum Computation and Quantum Information: 10th Anniversary edition* (Cambridge: Cambridge University Press)
[2] Yao N Y *et al* 2011 *Phys. Rev. Lett.* **106** 040505 and references therein
Yao N Y *et al* 2012 *Nat. Commun.* **3** 800
Yao N Y *et al* 2013 *Phys. Rev.* A **87** 022306
Weimer H *et al* 2013 *Phys. Rev. Lett.* **110** 067601
[3] Steger M *et al* 2012 *Science* **336** 1280
[4] Maurer P C *et al* 2012 *Science* **336** 1283
[5] Fleischhauer M *et al* 2000 *Opt. Commun.* **179** 395
[6] van der Wal C H *et al* 2003 *Science* **301** 196
[7] Hosseini M *et al* 2011 *Nat. Phys.* **7** 794
Novikova I *et al* 2012 *Laser Photonics Rev.* **6** 333
[8] Ciccarello F *et al* 2010 *Phys. Rev.* A **81** 042318
[9] Ping Y *et al* 2011 *New J. Phys.* **13** 103004
[10] Ziman M *et al* 2002 *Phys. Rev.* A **65** 042105
[11] Schrader D *et al* 2004 *Phys. Rev. Lett.* **93** 150501
[12] Jaksch D 2007 *Contemp. Phys.* **45** 367
[13] Breuer H-P and Petruccione F 2002 *The Theory of Open Quantum Systems* (Oxford: Oxford University Press)
[14] Beals R and Wong R 2010 *Special Functions* (Cambridge: Cambridge University Press)
[15] Bergamini S *et al* 2004 *J. Opt. Soc. Am.* B **21** 1889
[16] Boyer V *et al* 2006 *Phys. Rev. A* **73** 031402
[17] Beugnon J *et al* 2007 *Nat. Phys.* **3** 696
[18] Karski M *et al* 2009 *Science* **325** 174
[19] Bakr W S *et al* 2009 *Nature* **462** 74
[20] Sherson J F *et al* 2010 *Nature* **467** 68
[21] Weitenberg C *et al* 2011 *Nature* **471** 319
[22] Weber M *et al* 2006 *Phys. Rev. A* **73** 043406
[23] Grünzweig T *et al* 2010 *Nat. Phys.* **6** 951
[24] Brandt L *et al* 2011 *Appl. Phys.* B **102** 443
Muldoon C *et al* 2012 *New J. Phys.* **14** 073051 and references therein
[25] Trotzky S *et al* 2008 *Science* **319** 295
[26] Boyd M M *et al* 2006 *Science* **314** 1430
[27] Hewson A C 1993 *The Kondo Problem to Heavy Fermions* (Cambridge: Cambridge University Press)
[28] Duan L-M *et al* 2003 *Phys. Rev. Lett.* **91** 090402
[29] Jafarov E I and van der Jeugt J 2010 *J. Phys. A: Math. Theor.* **43** 405301
van der Jeugt J 2011 *J. Phys.: Conf. Ser.* **284** 012059
[30] Liu Z 2003 *Appl. Math. Comput.* **141** 297